DOI: 10.1002/chem.200902166

# A Quadruplex-Based, Label-Free, and Real-Time Fluorescence Assay for RNase H Activity and Inhibition

**Dan Hu, Fang Pu, Zhenzhen Huang, Jinsong Ren,* and Xiaogang Qu[a]**

**Abstract:** We demonstrate a unique quadruplex-based fluorescence assay for sensitive, facile, real-time, and label-free detection of RNase H activity and inhibition by using a G-quadruplex formation strategy. In our approach, a RNA–DNA substrate was prepared, with the DNA strand designed as a quadruplex-forming oligomer. Upon cleavage of the RNA strand by RNase H, the released G-rich DNA strand folds into a quadruplex in the presence of monovalent ions and interacts with a specific G-quadruplex binder, *N*-methyl mesoporphyrin IX (NMM); this gives a dramatic increase in fluorescence and serves as a reporter of the reaction. This novel assay is simple in design, fast in operation, and is more convenient and promising than other methods. It takes less than 30 min to finish and the detection limit is much better or at least comparable to previous reports. No sophisticated experimental techniques or chemical modification for either RNA or DNA are required. The assay can be accomplished by using a common spectrophotometer and obviates possible interference with the kinetic behavior of the catalysts. Our approach offers an ideal system for high-throughput screening of enzyme inhibitors and demonstrates that the structure of the G-quadruplex can be used as a functional tool in specific fields in the future.

**Keywords:** fluorescent probes · high-throughput screening · inhibitors · quadruplex DNA · RNase H

## Introduction

RNase H is a ribonuclease that can specifically degrade the RNA strand of an RNA–DNA duplex through an endonucleolytic mechanism.[1] Members of the RNase H family can be found in virtually all organisms, from archaea and prokaryota to eukaryota. The specific actions of these enzymes are essential in a variety of fields ranging from biotechnology to pharmacology, and in important cellular processes including DNA replication, DNA repair, and transcription.[2] Moreover, it is clear that RNase H activity of the multifunctional HIV-1 reverse transcriptase (RT) is absolutely required for completion of retroviral DNA synthesis, thereby rendering this function an attractive target for anti-HIV therapeutics.[3] In contrast with HIV-1-RT DNA polymerase inhibitors, very few RT-RNase H inhibitors have been identified.[4–10] The paucity of RNase H inhibitors is due in part to the cumbersome nature of the assays used to measure RNase H activity. Traditional techniques, including gel electrophoresis, high-performance liquid chromatography (HPLC), electrochemical studies, and the acid-soluble release of RNA fragments have been established in assays of enzyme activities and evaluations of the kinetic parameters.[11–14] These protocols share the drawbacks of being time-intensive, discontinuous, and laborious, and usually require isotope labeling. Many of these limitations are now being addressed by the development of fluorescence assays based on resonance energy transfer (FRET) or an excimer mechanism.[2,15–17] Although promising, these techniques are compromised by the requirement for double-labeled oligonucleotide substrates, limited chemical stability, and interference by external nonspecific events. In addition, the possibility that the bulky fluorescent groups might interfere with the kinetic behavior of the catalysts is always a concern. Very recently, a gold nanoparticle–RNA–fluorescent dye conjugate has been used for the detection of RNase H activity.[18] However, the need for functionalized thiol and dye-modified oligonucleotide probes added to the complexity,

[a] D. Hu, F. Pu, Z. Huang, Prof. Dr. J. Ren, Prof. Dr. X. Qu
Laboratory of Chemical Biology and
State Key laboratory of Rare Earth Resources Utilization
Changchun Institute of Applied Chemistry
Chinese Academy of Sciences
Changchun, 130022 (PR China)
Fax: (+86) 0431-85262625
E-mail: jren@ciac.jl.cn
and
Graduate School of the Chinese Academy of Sciences
Beijing, 100039 (PR China)

Supporting information for this article is available on the WWW under http://dx.doi.org/10.1002/chem.200902166.

   

cost, and overall assay time, and limited the effectiveness of such detection strategies.

## Results and Discussion

Herein, we demonstrated a new concept that overcomes these limitations by achieving a simple, fast, and label-free fluorescence assay for real-time detection of RNase H activity and inhibition by using a G-quadruplex as a functional tool. *N*-Methyl mesoporphyrin IX (NMM) is a commercially available unsymmetrical anionic porphyrin characterized by a pronounced structural selectivity for G-quadruplexes but not for duplexes (DNA, RNA, and RNA–DNA hybrids), triplexes, or single-stranded forms.[19,20] It is weakly fluorescent, but exhibits a $>20$-fold enhancement in its fluorescence upon binding to quadruplex DNA (with excitation and emission wavelengths centered at $\lambda = 399$ and 614 nm, respectively). However, similar properties were not at all evident in the presence of duplex, triplex or single-stranded nucleic acid structures. Our approach toward sensing RNase H is based on the unique fluorescence increase that occurs as a result of the strong interaction between NMM and the folded quadruplex upon cleavage by RNase H. As shown in Scheme 1, the DNA strand of the substrate was designed as a quadruplex-forming oligomer. In the absence of RNase H, the DNA and RNA oligomers exists in aqueous solution in a hybrid duplex structure. Because the interactions between the hybrid duplex and NMM are very weak, the fluorescence of such a mixture is weak. In the presence of RNase H, upon cleavage of RNA strand, the released G-rich strand folds into a quadruplex structure in the presence of monovalent ions. Because NMM can specifically interact with G-quadruplex DNA, the NMM–quadruplex complex fluoresces more strongly than free NMM. Thus, NMM serves as a reporter and one can monitor cleavage by the changes in fluorescence intensity.

G-rich oligonucleotides can be very polymorphic, and the structures that are adopted depend on several factors, including base sequence, strand concentration, loop connectivities, and cations present. The DNA strands can assemble together in either intramolecular (when a single strand folds upon itself) or intermolecular (when two or more strands associate) configuration.[21–25] NMM was reported to interact with a variety of quadruplex forms; among them, the dimeric G-quadruplex of $d(G_4T_4G_4)$, which consists of 1.5 units of the *Oxytricha nova* telomere repeat DNA sequence, gave the best fluorescence enhancement.[20] Because the kinetic analysis of various DNA quadruplexes indicates that the folding process of intramolecular structures are faster than intermolecular ones,[26,27] we extended the length of $d(G_4T_4G_4)$ to get various intramolecular G-quadruplexes. Interestingly, much higher fluorescence enhancement was obtained with these intramolecular quadruplexes, of which $d[G_3(T_4G_3)_3]$ was the highest (Figure 1A). Thus, the $d[G_3(T_4G_3)_3]$ sequence was chosen as the DNA strand of the hybrid substrate. CD spectra and UV melting analyses of $d[G_3(T_4G_3)_3]$ in buffer solutions, which differed only in their salt components, indicate that the sequence folds into a quadruplex structure under our experimental conditions (see Figure S1 in the Supporting Information), and fluorescence spectra also confirm the above results (see Figure S2 in the Supporting Information).

Steady-state fluorescence measurements were carried out to serve as a proof of concept to test the principle of our design. Fluorescence titration experiments were first performed in the presence of $d[G_3(T_4G_3)_3]$ quadruplex and $d[G_3(T_4G_3)_3]$–$r[C_3(A_4C_3)_3]$ hybrid duplex. The fluorescence signals increased promptly as the NMM concentration was increased, and little change was observed when the concen-

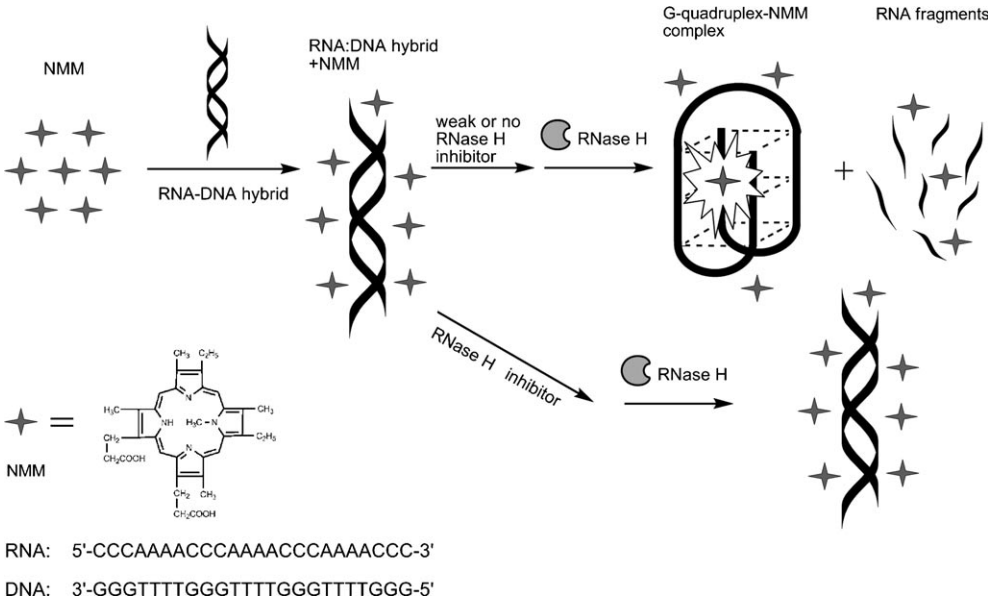


Scheme 1. Schematic illustration of the label-free assay for RNase H activity and inhibition, showing the molecular structure of NMM and the sequences of the RNA–DNA substrate. The DNA strand could form an intramolecular G-quadruplex with three $T_4$ loops.

  

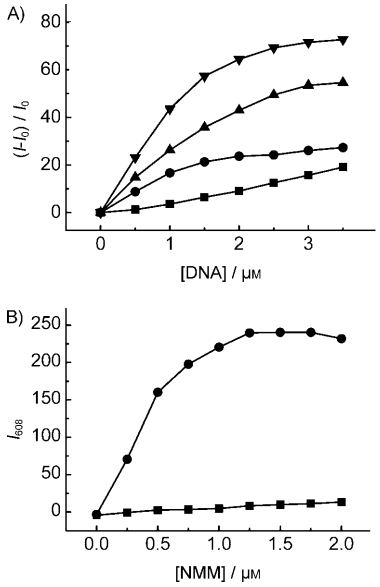


Figure 1. A) Fluorescence titration of NMM ($2\times10^{-6}$ M) with d[$G_4T_4G_4$] (■), d[$G_3(T_3G_3)_3$] (●), d[$G_4(T_4G_4)_3$] (▲), d[$G_3(T_4G_3)_3$] (▼). B) Fluorescence titration of the RNA–DNA hybrid (■) and DNA strand (●) with NMM. Experiments were carried out in a buffer containing 10 mM Tris–HCl, 100 mM NaCl, 10 mM KCl, 10 mM $MgCl_2$, pH 7.5.

tration exceeded 1 μM (Figure 1B). Therefore, 1 μM NMM was used in the experiments to ensure a good signal-to-background ratio. As can be seen in Figure 2, the fluorescence intensity of NMM alone or in the presence of RNA–DNA hybrid is very weak in 10 mM Tris–HCl, 100 mM NaCl, 10 mM KCl, 10 mM $MgCl_2$, pH 7.5 (Figure 2, curve a and b, excited at $\lambda=399$ nm, emission at $\lambda=608$ nm); this supports the notion that the RNA–DNA hybrid interacts weakly with NMM. However, a significant increase (18-fold) in fluorescence intensity was observed upon addition of RNase H to the mixture (Figure 2, curve c). Moreover, the cleavage reaction appeared to be nearly complete because the final fluorescence value is very close to the emission intensity expected for NMM bound to the same amount of d[$G_3(T_4G_3)_3$] (Figure 2, curve d). Meanwhile, a common substrate, polyA•polydT, was used to test the possible inhibitory effect of NMM on RNase H activity. The time curves of cleavage of

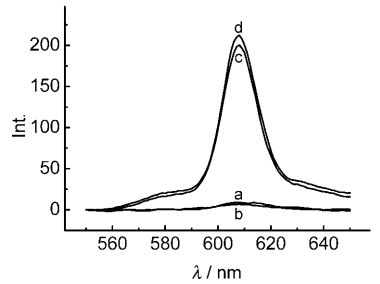


Figure 2. Fluorescence spectra of solutions containing a) NMM, b) NMM/RNA–DNA hybrid in the absence of *E. coli* RNase H, c) NMM/RNA–DNA hybrid in the presence of *E. coli* RNase H, and d) NMM/DNA, upon excitation of $\lambda=399$ nm. [NMM] $=1\times10^{-6}$ M, [DNA or RNA–DNA hybrid] $=5\times10^{-7}$ M.

polyA•polydT by RNase H (see Figure S3 in the Supporting Information) are identical in the absence or presence of 2 μM NMM; this demonstrates that NMM does not inhibit the digestion of the RNA–DNA hybrid by the nuclease. Furthermore, the association rate of NMM with the G-quadruplex was determined with a $\tau$ of 21 s (see Figure S4 in the Supporting Information), which is much faster than the enzymatic reaction rate and would not limit the observed kinetics. Therefore, our approach can be applied to monitor real-time RNA strand cleavage and provide information about the dynamics of the cleavage process.

The fluorescence intensity at $\lambda=608$ nm, which is associated with the population of released DNA, was then studied as a function of incubating time. Figure 3A shows the time

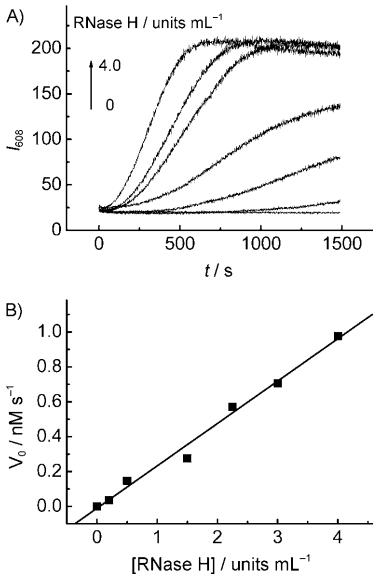


Figure 3. A) The fluorescence intensity of NMM at $\lambda=608$ nm vs. digestion time of RNA by various concentrations of *E. coli* RNase H at 25 °C. [RNA–DNA hybrid] $=5\times10^{-7}$ M. B) Initial cleavage velocity as a function of the concentration of *E. coli* RNase H.

curves of the digestion reaction with various concentrations of RNase H from 0.2 to 4.0 units $mL^{-1}$. The rapid increase in fluorescence clearly shows that the formation of a G-quadruplex–NMM complex can be attributed only to the cleaving of the substrate and liberation of the G-quadruplex-forming strand by RNase H because the fluorescence of the substrate remained constant over the period without RNase H under the same experimental conditions. In addition, we carried out control experiments with different concentrations of monovalent cations. As can be seen in Figures S1 and S2 in the Supporting Information, d[$G_3$ ($T_4G_3$)$_3$] could not fold into a stable quadruplex in the absence of monovalent cations. As a consequence, almost no fluorescence change was observed upon addition of *Escherichia coli* RNase H (see Figure S5A in the Supporting Information). Interestingly, a large fluorescence increase, which is close to the value obtained in Mg/Na/K buffer, was observed when 10 mM KCl

  

was added to the cleavage product (see Figure S5B in the Supporting Information). The results demonstrated the necessity of monovalent cations in G-quadruplex formation and further supported our proof-of-concept assay. The slopes of the curves decreased gradually over time, which indicated that RNase H cleavage slowed as the substrate was consumed. It was found that the fluorescence intensity reached a plateau after 20 min, which indicated that the digestion was nearly completed. It is possible to detect enzyme activity within 5–10 min, which shows one of the advantages of the quick response of the system. The reaction rate increased with increasing enzyme concentration, and the initial digestion rate can be measured from the linear portion of the time curve. A good linear relationship was observed between initial digestion rate and enzyme concentration (Figure 3B), which indicates that the cleavage reaction is first order with respect to RNase H concentration and is consistent with the general model for enzyme-catalyzed reactions.[28] The detection limit herein (0.2 units $mL^{-1}$) is much lower than the value obtained with the pyrene–pyrene excimer assay.[17] Furthermore, more sensitive detection could be achieved by optimizing the G-quadruplex-forming sequence and the cleavage conditions, for example, increasing the concentration of substrates or prolonging the cleavage time.

To further confirm the validity of the NMM–quadruplex-based method, the relationship between the initial digestion rate and substrate concentration was studied. As shown in Figure 4, the initial digestion rate increases with an increase in substrate concentration, [S]. The initial cleavage rate, $V_0$, was measured from the time curves. Plotting $1/V_0$ versus 1/[S] gives a straight line (the Lineweaver–Burk plot). Values for several important kinetic parameters were obtained: 1.64 nM $s^{-1}$ for the maximum initial velocity ($V_{max}$), 288 nM for the Michaelis–Menten constant ($K_M$), and 3.42 $s^{-1}$ for the turnover number ($k_{cat}$). $K_M$ for RNase H has been reported to vary from 19 to 4.2 μM.[2,12,17,29] The variation is the result of a variety of assay conditions, substrates, and methods.

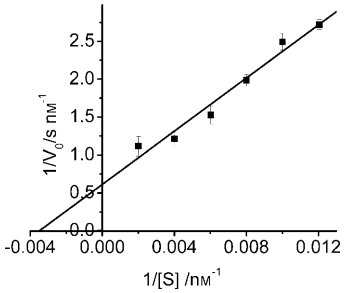


Figure 4. Lineweaver–Burk plot of the reciprocals of initial rate vs. substrate concentration for the determination of kinetic parameters $K_M$, $k_{cat}$, and $V_{max}$ of RNase H in the quadruplex-based assay. From the linear fit of the data, we determined $K_M = 288$ nM, $V_{max} = 1.64$ nM $s^{-1}$, and $k_{cat} = 3.42$ $s^{-1}$ ($y = 0.61 + 175.48x$, $R = 0.98$). Reaction conditions: [RNA–DNA hybrid] = 83, 100, 125, 166, 250, 500 nM, [*E. coli* RNase H] = 4.0 units $mL^{-1}$. Error bars were estimated from at least three independent measurements.

Moreover, diverse RNase H proteins from various sources, such as human RNase H1, *E. coli* RNase H, and HIV-1-RT, share structural similarities but differ in some of their functional properties. For example, the RNase H domain of HIV-1-RT requires the polymerase domain for RNA degradation,[30] whereas the RNase H domain of human RNase H1 alone shows significant activity,[31] as does *E. coli* RNase H. These differences prompt us to ask whether the particular RNA–DNA hybrid substrate that was used in our method is not only for *E. coli* RNase H but also for other RNase H proteins. To address the general approach for RNase H, detection of HIV-1-RT-associated RNase H activity was further studied. HIV-1-RT-associated RNase H is among the novel non-traditional targets that have been investigated to identify new HIV inhibitors. Our results demonstrate that this enzyme could also recognize and cleave the hybrid duplex. Cleavage of the RNA strand results in the fluorescence enhancement of NMM (Figure 5).

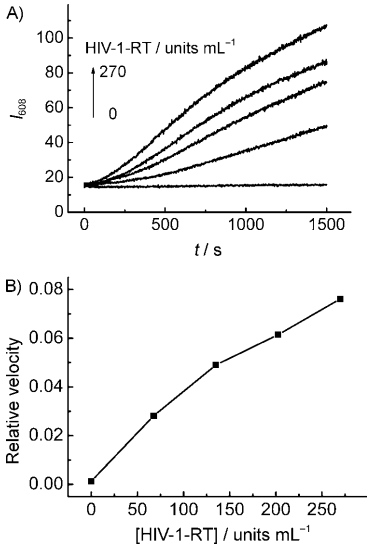


Figure 5. A) The fluorescence intensity of NMM at $\lambda = 608$ nm vs. digestion time of RNA by various concentrations of HIV-1-RT-associated RNase H at 37 °C. [RNA–DNA hybrid] = $5 \times 10^{-7}$ M. B) Initial cleavage velocity as a function of the concentration of HIV-1-RT.

RNase H proteins represent an exciting and novel family of targets, and the pharmacological inhibition of RNase H provides a broad spectrum of therapeutic applications, including but not limited to anticancer, antiviral drugs, and in particular, anti-HIV therapeutics. For instance, RNase H functions associated with the viral reverse transcriptase (RT) that hydrolyzes the RNA of the RNA–DNA replication intermediate is among the novel, non-traditional, targets that have been investigated to identify new HIV inhibitors. In fact, several studies have demonstrated that the abolition of this enzyme function stops virus replication and that, therefore, it is an attractive target for drug development.[3] However, RNase H is a drug target that has been little explored so far due in part to the cumbersome nature

  

of the assays used to measure RNase H activity. The NMM–quadruplex-based approach can also be applied to screen RNase H inhibitors. Two small molecules, ellipticine and ethidium bromide, were selected for our studies. Ellipticine and ethidium bromide (EB) have been identified to preferentially target RNA–DNA hybrid duplexes and effectively inhibit RNase H activity at micromolar concentrations.[32] In the inhibition assay, a solution of the RNA–DNA hybrid duplex and the inhibitors of varying concentrations were incubated at 25 °C for 15 min, then NMM and *E. coli* RNase H were added and the mixtures were left for 10 min to allow hydrolysis to occur. The $IC_{50}$ value (the inhibitor concentration required to reduce enzyme activity by 50 %) was obtained from the plot of relative activity (RA) versus inhibitor concentration (Figure 6). Ellipticine and EB were found to inhibit *E. coli* RNase H with $IC_{50}$ values of 2.85 and 5.1 μM, respectively. These results are in good agreement with the reported literature value determined by other methods.[32]

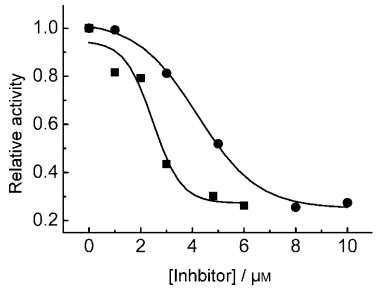


Figure 6. Inhibition efficiency of *E. coli* RNase H activity by ellipticine (■) and EB (●). The $IC_{50}$ values were obtained from the curve.

Considering the diversity of RNase H proteins and the differences in some of their functional properties, inhibitors selected for one kind of enzyme might have no effect on another. As was stressed by Pileur et al., the selected aptamers in their study were specific inhibitors for the eukaryotic RNase H1 but ineffective against *E. coli* RNase H and HIV-1-RT RNase H despite the common structural properties of these three enzymes.[33] To test whether the small molecules against *E. coli* RNase H are effective inhibitors against HIV-1-RT-associated RNase H, ellipticine was chosen due to its efficiency on *E. coli* RNase H. Our result demonstrates that ellipticine can inhibit HIV-1-RT RNase H with an inhibition efficiency of 70 % at 10 μM (see Figure S6 in the Supporting Information). This feature of small-molecule inhibitors targeting a RNA–DNA hybrid is consistent with previous reports.[9,34] More importantly, these low-molecular-weight inhibitors highlight a potential strategy for AIDS chemotherapy that should not be compromised by the unusual genetic diversity of HIV-1 as demonstrated by Li et al.[9] Thus, the methodology described herein provides a simple, sensitive, and rapid protocol for screening RNase H inhibitors and anti-HIV drugs.

## Conclusion

In summary, we have demonstrated a unique quadruplex-based, fluorescence assay for the sensitive, facile, real-time, and label-free detection of RNase H activity and inhibition. The method relies on the large fluorescence enhancement through specific binding of the small molecule NMM with G-quadruplex DNA. The assay technique has several important features. The assay presented herein is simple in design and offers a convenient "mix-and-detect" protocol for homogeneous, ratiometric, and rapid detection with high sensitivity. It takes less than 30 min to perform and the detection limit is much better than or at least comparable to previously reported methods. In addition, sophisticated experimental techniques are not required. The assay can be accomplished by using a common spectrophotometer. More importantly, this approach does not require any chemical modification of either the RNA or DNA, which offers the advantages of simplicity and cost efficiency and obviates possible interference with the kinetic behavior of the catalysts. Finally, the approach offers an ideal system for high-throughput screening of enzyme inhibitors and illustrates that the structure of G-quadruplex could be used as a functional tool. We expect that this strategy will have important applications in a wide range of biological and biomedical processes, especially in the screening of anti-HIV therapeutics.

## Experimental Section

**Materials and measurements**: DNA: 5′-GGG-TTT-TGG-GTT-TTG-GGT-TTT-GGG-3′, RNA: 5′-CCC-AAA-ACC-CAA-AAC-CCA-AAA-CCC-3′ were synthesized by AuGCT Biotechnology (Beijing, China). All other oligonucleotides were synthesized by Shanghai Sangon Biological Engineering Technology & Services (Shanghai, China). *E. coli* RNase H with an enzyme activity of $6\times10^4$ units $mL^{-1}$ was purchased from Takara Biotechnology (Dalian, China). Recombinant HIV-1-RT, with an enzyme activity of 27.0 units $\mu L^{-1}$ was purchased from Worthington Biochemical Corporation (Lakewood, NJ, USA), NMM was purchased from Porphyrin Products (Logan, UT), and its concentration was measured by using absorbance spectroscopy on a JASCO V-550 and found to be $\lambda = 379$ nm, assuming an extinction coefficient of $1.45\times10^5\,M^{-1}\,cm^{-1}$. Other chemicals were purchased from Sigma–Aldrich and used without further purification. All water used to prepare buffer solutions was obtained by using a Milli-Q water system.

Steady-state fluorescence measurements and time curves were carried out by using a JASCO FP-6500 spectrofluorometer with the temperature held at 25 °C for *E. coli* RNase H and 37 °C for HIV-1-RT by an aqueous thermostat. The fluorescence intensity of all samples was analyzed by a time base scan ($\lambda_{ex} = 399$ nm, $\lambda_{em} = 608$ nm). Slit widths for the excitation and emission were set at 5 and 10 nm, respectively. All measurements were performed in 10 mM Tris–HCl, 100 mM NaCl, 10 mM KCl, 10 mM $MgCl_2$, pH 7.5 (Mg/Na/K buffer) for *E. coli* RNase H and 20 mM Tris–HCl, 10 mM KCl, 10 mM $MgCl_2$, 1 mM $Na_2EDTA$, pH 8.0 for HIV-1-RT. The Mg buffer and Mg/Na buffer that were used for control analysis differ in their lack of corresponding salt components compared with Mg/Na/K buffer. Stopped-flow fluorescence measurements were performed at 25 °C under standard buffer conditions by using a stopped-flow device from Applied Photophysics (Leatherhead, Surrey, KT22 7PB, UK) in two-syringe mode.

**Assay for RNase H activity and inhibition**: Assays were carried out in 1× Mg/Na/K buffer (300 μL) that contained 500 nM RNA–DNA hybrid and

  

various amounts of *E. coli* RNase H. For determination of the Michaelis–Menten kinetics parameters, the hybrid concentration was varied from 83 to 500 nM, over the range of the previous reported $K_M$ values for RNase H. All experiments were performed at 25 °C and repeated at least three times. The initial rate of the cleavage reaction was determined by linear regression of the initial parts of the fluorescence scan curves. Assays for HIV-1-RT-associated RNase H activity were carried out in the corresponding buffer (200 μL) that contained 500 nM RNA–DNA hybrid and various amounts of HIV-1-RT at 37 °C.

For the *E. coli* RNase H inhibition assay, a total volume of 300 μL reaction solution that contained RNA–DNA hybrid (500 nM) and various amounts of drug (ellipticine or ethidium bromide) were incubated at 25 °C for 15 min in a 0.5 mL Eppendorf tube, then NMM (1 μM) and *E. coli* RNase H (4.0 unit $mL^{-1}$) were added into the tube. The fluorescence time curves were measured immediately in a 500 μL quartz cuvette at 25 °C. The activity of *E. coli* RNase H was also obtained by measuring the initial reaction velocity.

## Acknowledgements

This work was supported by NSFC (grant nos. 20831003, 90913007, 90813001, and 20833006) and funds from the Chinese Academy of Sciences and Jilin Province.

[1] *Ribonuclease H* (Eds.: R. J. Crouch, J. J. Toulme), Libbey, Paris, **1998**.
[2] J. Rizzo, L. K. Gifford, X. Zhang, A. M. Gewirtz, P. Lu, *Mol. Cell. Probes* **2002**, *16*, 277–283.
[3] G. J. Klarmann, M. E. Hawkins, S. F. Le Grice, *AIDS Res.* **2002**, *4*, 183–194.
[4] S. Loya and A. Hizi, *J. Biol. Chem.* **1993**, *268*, 9323–9328.
[5] G. Borkow, R. S. Fletcher, J. Barnard, D. Arion, D. Motakis, G. I. Dmitrienko, M. A. Parniak, *Biochemistry* **1997**, *36*, 3179–3185.
[6] S. Gabbara, W. R. Davis, L. Hupe, D. Hupe, J. A. Peliska, *Biochemistry* **1999**, *38*, 13070–13076.
[7] M. L. Andreola, F. Pileur, C. Calmels, M. Ventura, L. Tarrago-Litvak, J. J. Toulme, S. Litvak, *Biochemistry* **2001**, *40*, 10087–10094.
[8] C. A. Shaw-Reid, V. Munshi, P. Graham, A. Wolfe, M. Witmer, R. Danzeisen, D. B. Olsen, S. S. Carroll, M. Embrey, J. S. Wai, M. D. Miller, J. L. Cole, D. J. Hazuda, *J. Biol. Chem.* **2003**, *278*, 2777–2780.
[9] T. K. Li, C. M. Barbieri, H. C. Lin, A. B. Rabson, G. Yang, Y. Fan, B. L. Gaffney, R. A. Jones, D. S. Pilch, *Biochemistry* **2004**, *43*, 9732–9742.
[10] S. R. Budihas, I. Gorshkova, S. Gaidamakov, A. Wamiru, M. K. Bona, M. A. Parniak, R. J. Crouch, J. B. McMahon, J. A. Beutler, S. F. Le Grice, *Nucleic Acids Res.* **2005**, *33*, 1249–1256.
[11] E. Kanaya, S. Kanaya, *FEBS J.* **1995**, *231*, 557–562.
[12] H. H. Hogrefe, R. I. Hogrefe, R. Y. Walder, J. A. Walder, *J. Biol. Chem.* **1990**, *265*, 5561–5566.
[13] K. C. Chan, S. R. Budihas, S. F. Le Grice, M. A. Parniak, R. J. Crouch, S. A. Gaidamakov, H. J. Isaaq, A. Wamiru, J. B. McMahon, J. A. Beutler, *Anal. Biochem.* **2004**, *331*, 296–302.
[14] M. L. Dirksen, R. J. Crouch, *J. Biol. Chem.* **1981**, *256*, 11569–11573.
[15] M. A. Parniak, K. L. Min, S. R. Budihas, S. F. Le Grice, J. A. Beutler, *Anal. Biochem.* **2003**, *322*, 33–39.
[16] N. Potenza, V. Salvatore, A. Migliozzi, V. Martone, V. Nobile, A. Russo, *Nucleic Acids Res.* **2006**, *34*, 2906–2913.
[17] Y. Chen, C. J. Yang, Y. Wu, P. Conlon, Y. Kim, H. Lin, W. Tan, *ChemBioChem* **2008**, *9*, 355–359.
[18] J. H. Kim, R. A. Estabrook, G. Braun, B. R. Lee, N. O. Reich, *Chem. Commun. (Cambridge)* **2007**, 4342–4344.
[19] J. Ren, J. B. Chaires, *Biochemistry* **1999**, *38*, 16067–16075.
[20] H. Arthanari, S. Basu, T. L. Kawano, P. H. Bolton, *Nucleic Acids Res.* **1998**, *26*, 3724–3728.
[21] G. N. Parkinson, M. P. Lee, S. Neidle, *Nature* **2002**, *417*, 876–880.
[22] J. Ren, X. Qu, J. O. Trent, J. B. Chaires, *Nucleic Acids Res.* **2002**, *30*, 2307–2315.
[23] A. N. Lane, J. B. Chaires, R. D. Gray, J. O. Trent, *Nucleic Acids Res.* **2008**, *36*, 5482–5515.
[24] G. R. Clark, P. D. Pytel, C. J. Squire, S. Neidle, *J. Am. Chem. Soc.* **2003**, *125*, 4066–4067.
[25] D. Miyoshi, H. Karimata, Z. M. Wang, K. Koumoto, N. Sugimoto, *J. Am. Chem. Soc.* **2007**, *129*, 5919–5925.
[26] J. L. Mergny, A. De Cian, A. Ghelab, B. Sacca, L. Lacroix, *Nucleic Acids Res.* **2005**, *33*, 81–94.
[27] R. D. Gray, J. B. Chaires, *Nucleic Acids Res.* **2008**, *36*, 4191–4203.
[28] A. L. Lehninger, D. L. Nelson, M. M. Cox, *Principles of Biochemistry*, Worth Publishers, New York, **1993**, pp. 202–213.
[29] J. L. Keck, E. R. Goedken, S. Marqusee, *J. Biol. Chem.* **1998**, *273*, 34128–34133.
[30] Z. Hostomsky, Z. Hostomska, G. O. Hudson, E. W. Moomaw, B. R. Nodes, *Proc. Natl. Acad. Sci. USA* **1991**, *88*, 1148–1152.
[31] M. Nowotny, S. A. Gaidamakov, R. Ghirlando, S. M. Cerritelli, R. J. Crouch, W. Yang, *Mol. Cell* **2007**, *28*, 264–276.
[32] J. Ren, X. Qu, N. Dattagupta, J. B. Chaires, *J. Am. Chem. Soc.* **2001**, *123*, 6742–6743.
[33] F. Pileur, M. L. Andreola, E. Dausse, J. Michel, S. Moreau, H. Yamada, S. A. Gaidamakov, R. J. Crouch, J. J. Toulme, C. Cazenave, *Nucleic Acids Res.* **2003**, *31*, 5776–5788.
[34] C. M. Barbieri, T. K. Li, S. Guo, G. Wang, A. J. Shallop, W. Pan, G. Yang, B. L. Gaffney, R. A. Jones, D. S. Pilch, *J. Am. Chem. Soc.* **2003**, *125*, 6469–6477.

Received: August 4, 2009
Revised: November 17, 2009
Published online: January 14, 2010

  